Highly efficient delivery of p16 antitumor peptide into aggressive leukemia/lymphoma cells using a novel transporter system

Eisaku Kondo,[1] Masao Seto,[2] Kazuhiro Yoshikawa,[3] and Tadashi Yoshino[1]

[1]Department of Pathology, Okayama University Graduate School of Medicine and Dentistry, Okayama, Japan; [2]Division of Molecular Medicine, Aichi Cancer Center Research Institute, Nagoya, Aichi, Japan; and [3]Second Department of Pathology, Aichi Medical University School of Medicine, Nagakute, Aichi, Japan

Abstract

Molecular targeting of hematopoietic malignancies has been generally hindered by technological obstacles to gene delivery in the neoplastic cells. The development of peptide delivery systems based on protein transduction domains has recently gained attention as a means of potentially overcoming these impediments. Here, we present a novel peptide transporter system that increases the efficiency of peptide delivery more than 10 times compared with the previous methods. The transporter, Wr-T, has an enlarged hydrophobic pocket consisting of triple tryptophan-rich domains fused with nine D-enantiomer polyarginines (r9) via Gly-Pro-Gly spacer, which serves to augment delivery of a cargo peptide. Wr-T–mediated transport of $p16^{INK4a}$ functional peptide dramatically inhibits growth of highly aggressive leukemia/lymphomas by up to 80% through restoration of p16 function. The Wr-T system thus represents a highly effective approach to cargo peptide delivery with the potential for substantially developing p16 peptide–based therapy for hematopoietic malignancies. [Mol Cancer Ther 2004;3(12):1623–30]

Introduction

Hematopoietic malignancies including the leukemia/lymphomas have been remarkably unyielding to gene transfer modalities, and hence there is a keen interest in advancements to the fields of gene/gene product delivery. Recent studies have identified various protein transduction domain sequences such as HIV-1 TAT, pAntp43-58, polyarginine (R4–16), and several nuclear localization signals that have been used in peptide/protein delivery systems (1–5). Protein transduction domain systems have been theoretically preferred to other systems such as recombinant viruses on the grounds of reduced *in vivo* pathogenicity, immunogenicity, and cytotoxicity. In addition to intracellular delivery systems of directly protein transduction domain–conjugated oligopeptides, the peptide/protein transporter system has also been reported as a more advanced protein transduction domain system, which has a wider choice of peptide/protein as a cargo (6). For example, Pep-1, the transporter having SV40 nuclear localization signal as a part of it, showed intracellular delivery of oligopeptides, recombinant proteins, and antibodies into several kinds of mammalian cells (6). Thus, several protein transduction domain systems have merged; however, these are not as yet sufficiently efficacious to have come into full practice, and there were few reports that specifically showed/ the examples of molecular targeting focused on hematopoietic malignancies using protein transduction domain systems. Accordingly, we have developed a high-peformance peptide delivery system for hematopoietic cells using a functionally reinforced peptide transporter and challenged growth suppression of highly aggressive leukemia/lymphomas by restoring p16 function via the novel transporter/p16 functional peptide delivery system.

Materials and Methods

Peptide Synthesis

All peptides including Wr-T, WR-T, r9-p16 minimal inhibitory sequence (MIS), and Pep-1 in the present study were synthesized at Sigma Genosys Co. Ltd. (Sapporo, Japan) by standard Fmoc chemistry on an ABI 433A peptide synthesizer (Applied Biosystems, Foster City, CA). Crude peptides were purified by reverse-phase high-performance or high-pressure liquid chromatography over a C18 preparatory column (Varian, Palo Alto, CA). The identity of all peptides was confirmed by mass spectrometry. All peptides precipitated from trifluoroacetic acid solutions are trifluoroacetic acid salts. We prepared the HCl form of peptides following high-performance liquid chromatography purification for *in vitro* and *in vivo* applications. The amino acid sequences of the transporters Wr-T and WR-T are KETWWETWWTEWWTEWSQGPGrrrrrrrrr (r, D-enantiomer arginine) and KETWWETWWTEWW-TEWSQGPGRRRRRRRRR, respectively. For synthesis of p16 MIS, the 10 sequential amino acid residues ''FLDTLVVLHR,'' identified as the MIS of p16 by Fahraeus et al. (7), was defined as the functional core of the peptide, which is insoluble, as is the entire p16 molecule (MIS hydrophobicity, 69.2%). We therefore fused r9 to these 10 amino acids to make the conjugate less hydrophobic (hydrophobicity, 40%), thus facilitating introduction into cells. r9-p16 MIS peptide was FITC-labeled at its NH_2

Received 6/21/04; revised 9/8/04; accepted 9/28/04.

The costs of publication of this article were defrayed in part by the payment of page charges. This article must therefore be hereby marked advertisement in accordance with 18 U.S.C. Section 1734 solely to indicate this fact.

Requests for reprints: Eisaku Kondo, Department of Pathology, Okayama University Graduate School of Medicine and Dentistry, 2-5-1 Shikata-cho, Okayama 700-8558, Japan. Phone: 81-86-235-7151; Fax: 81-86-235-7156. E-mail: ekondo@md.okayama-u.ac.jp

terminus of the amino acids for fluorescence microscopic and flow cytometric analyses; unlabeled p16 peptide was used for other biological assays. Pep-1 transporter was synthesized following the sequence reported by Morris et al. (6): Pep-1, KETWWETWWTEWSQPKKKRKV.

Peptide Transduction

For introduction of the peptide mixture *in vitro* growth suppression, the Wr-T peptide and r9-p16 MIS peptide were mixed in 50 μL of PBS at room temperature for 45 minutes (final concentration: Wr-T, 5 μmol/L; r9-p16 MIS, 2 μmol/L). The solution was then added directly to 500 μL of RPMI 1640 containing 10% fetal bovine serum to obtain the indicated final concentration.

In vivo peptide delivery to solid human Burkitt's tumor was done as follows: the Wr-T/r9-p16 MIS peptide mix (Wr-T, 40 nmol; r9-p16 MIS, 20 nmol) was s.c. injected so as to surround the whole tumor when it had grown to a diameter of 3 mm (tumor volume, ~100 mm^3). For the control groups, in parallel, 100 μL of PBS without peptide or Wr-T peptide alone was dissolved in 100 μL of PBS and injected into mice.

Cells

Human mantle cell lymphoma cell line SP-53 carrying t(11;14) (kindly provided by Y. Ohtsuki, Kochi University Medical School), Burkitt's lymphoma cell line BALM-14 and BALM-18 [both bearing t(8;14)], acute lymphoblastic leukemia cell line BALL-1, chronic myeloblastic leukemia cell line K-562 carrying t(9;22), and a natural killer lymphoma cell line YT were maintained in RPMI 1640 plus 10% fetal bovine serum at 37°C in a 5% CO_2 incubator (8–11). DERL-2, which exhibits the immune cell phenotype of natural killer-T-cell leukemia/lymphoma, was maintained in RPMI 1640 plus 10% fetal bovine serum containing 100 units/mL of interleukin 2 (11). BALM-14, BALM-18, BALL-1, K-562, YT, and DERL-2 were kindly provided by Fujisaki Cell Center, Hayashibara Biochemical Institute, Japan. Primary Burkitt's lymphoma cells were freshly isolated from the pleural effusion of a patient in the advanced stages of lymphoma. The number of viable cells in each cell line was assessed by counting trypan blue–excluding cells on a hemocytometer. Results show the average of three counts for each value. Informed patient consent was obtained for use of the primary lymphoma cells in this study.

Flow Cytometry

For fluorescence intensity measurements, cells treated with FITC-labeled peptides were washed thrice with PBS, then immediately analyzed by FACScan and Cell Quest software (Becton Dickinson, Palo Alto, CA). Cell cycle analysis was done using FACScan on cells whose DNA was stained with 10 μg/mL propidium iodide in 0.5% NP40 24 hours after introduction of the peptides, according to the manufacturer's staining protocol (Qbiogene, Carlsbad, CA). Apoptosis assays were done with the Cy-3 Annexin V staining kit (MBL Co. Ltd., Nagoya, Japan) on the peptide-treated cells following the manufacturer's instructions followed by FACScan analysis.

Fluorescence Microscopy and Confocal Laser Scanning Microscopy

Uptake and intracellular localization of FITC-labeled r9-p16 MIS peptide or FITC-labeled Wr-T peptide were assessed by both inverted fluorescence microscope (Olympus IX71-ARCEVA, Tokyo, Japan) and confocal laser scanning microscopy (LSM510, Zeiss, Jena, Germany). Inverted fluorescence microscope was used for detecting FITC signal in living SP-53 cells, peripheral blood mononuclear cells (PBMC), and primary lymphoma cells, cultured in RPMI 1640 supplemented with 10% fetal bovine serum. Nuclear localization of the FITC-conjugated peptide was determined by propidium iodide staining of RNase-treated cells and dual laser detection under confocal laser microscope. Living cells were washed thrice in RPMI 1640 with 10% fetal bovine serum prior to microscopic assays and were observed without fixation.

Reverse Transcription – PCR

Five micrograms of total RNA was extracted from each human leukemia/lymphoma cell line using RNA-Bee (TEL-TEST, Friendswood, TX). Subsequently, cDNA was synthesized from the extracted RNA using an oligo(dT) primer and cDNA synthesis kit (SuperScript first-strand synthesis system, Invitrogen, Carlsbad, CA). Reverse transcription-PCR was done by using Z-Taq polymerase (Takara Bio, Tokyo, Japan): amplification conditions were 98°C for 3 minutes followed by 26 cycles of a 98°C, 2-second denaturation with a 68°C, 15-second extension. A final brief extension was at 72°C. The sense/antisense primer sequences for *Cdk4*, *Cyclin D1*, and *GAPDH* were as described previously (12). The sense and antisense primer sequences for $p16^{INK4a}$ were 5′-ATGGAGCCGGCGGCGGGGAG-3′ and 5′-TCAATCGGGGATGTCTGAGG-3′, respectively.

Immunoblotting

Cells were promptly lysed with SDS sample buffer and the extracts were separated by SDS-PAGE using 4% to 12% bis-Tris gradient gels (Novex, San Diego, CA). Gels were blotted on nitrocellulose membrane, then sequentially probed with the following antibodies after blocking with Superblock (Pierce, Rockford, IL): rabbit polyclonal anti-phospho-Ser^{780} pRB (Cell Signaling Technology Inc., Beverly, MA) and anti-actin (Chemicon, Temecula, CA).

Mouse Tumor Models

Six-week-old BALB/c female nude mice were obtained from CLEA JAPAN, Inc. (Tokyo, Japan). A total of 1.0×10^7 cells of the BALM-14 human Burkitt lymphoma line, were taken up in 100 μL of RPMI 1640 and s.c. injected into each mouse to form a solid tumor nodule. Method of introduction of the peptide to the tumor was described above (see Peptide Transduction).

Results

Design and Intracellular Uptake of the Wr-T and the Cargo p16 Peptide

We first designed the transporter Wr-T based on Pep-1, which consists of an enlarged hydrophobic peptide-binding domain made by tripling a tryptophan-rich motif

(WWTE/ET) and by sequential fusion to a nine poly-D-arginine (r9) via a GPG spacer (Fig. 1A). Our theoretical expectation was that this expanded motif should increase the capacity for docking cargo peptides. In addition, the protein transduction domain, r9, was expected to exceed SV40 nuclear localization signal in cell permeability (3). We selected p16 as a molecular target for our Wr-T system because loss of p16 expression has been reported to be a hallmark of aggressive leukemia/lymphomas (13–15). We used a r9-fusion-p16 MIS (7) peptide (r9-p16 MIS) as a cargo peptide for Wr-T–mediated oligopeptide delivery (Fig. 1A). Cellular uptake of FITC-r9-p16 MIS by the peptide carriers was assessed using SP-53 cells, a human mantle cell lymphoma cell line (8). After 12 hours incubation with the Wr-T/p16 peptide mixture, we observed dramatic uptake of FITC-r9-p16 MIS, which was distributed throughout each living SP-53 cell (Fig. 1B). By comparison, r9-p16 MIS alone was transduced at much lower efficiency, and the transduced peptide showed a punctate vesicular pattern at the cytoplasms, which indicated endosomal localization (Fig. 1B). Using peptide transporters, Wr-T–mediated transport of r9-p16 MIS was more efficient than Pep-1 in a time-dependent manner (Fig. 1B). To examine differences in efficiency of a cargo peptide delivery by transporters, SP-53 cells were incubated for 12 hours with the mixture of FITC-r9-p16 MIS and each transporter (Pep-1, WR-T, or Wr-T; Fig. 1C), and the transduction was measured by fluorescence-activated cell sorting (FACS) analysis. More than 98% of the cells in each sample were positive for cellular uptake of r9-p16 MIS; however, we observed wide differences between the systems in terms of actual transduction efficiencies in

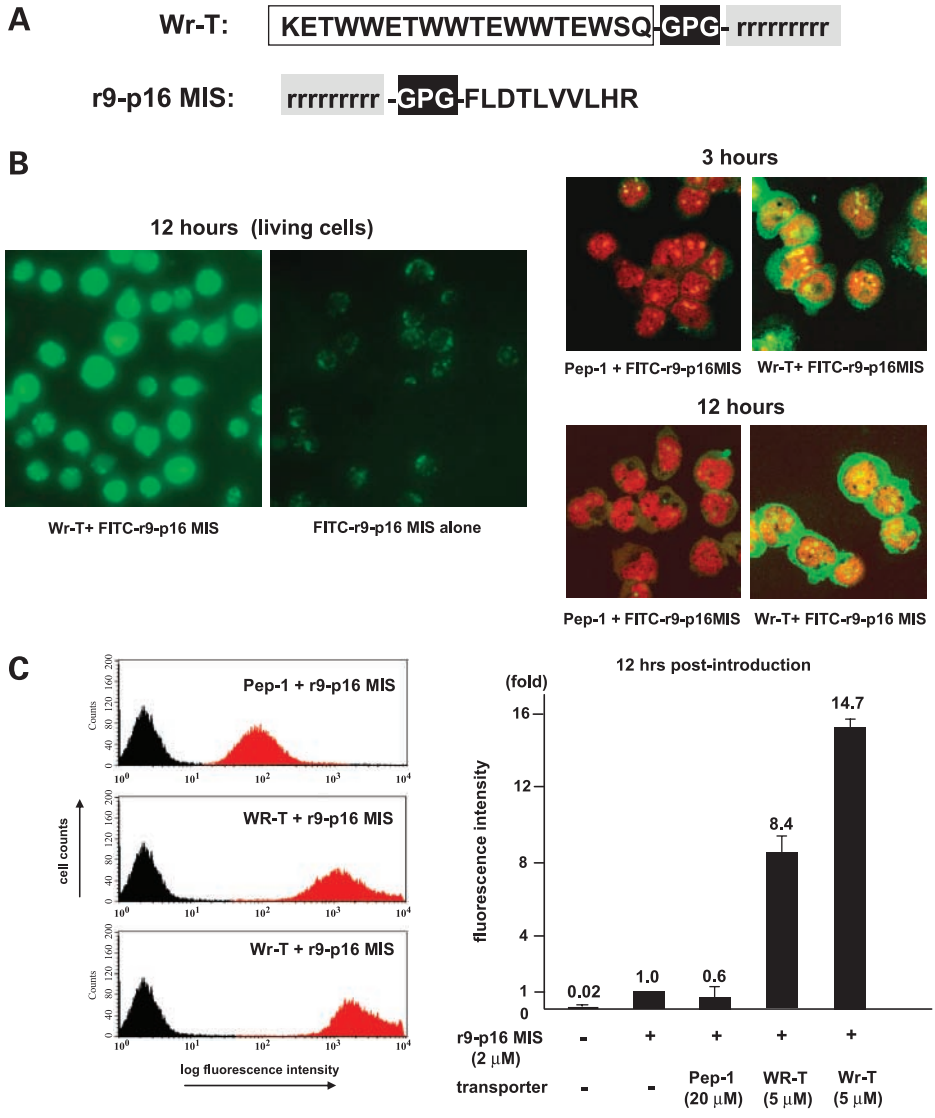

Figure 1. Cellular uptake of FITC-labeled p16 MIS by the Wr-T transporter. **A,** sequences of the Wr-T peptide-transporter and r9-p16 inhibitory peptide that contains the functional amino acid sequence of p16 (p16 MIS). *Open box,* hydrophobic peptide-binding domain; *black box,* spacer region; *gray box,* protein transduction domain. *r,* D-arginine; *R,* L-arginine. **B,** fluorescence images of incorporated FITC-labeled r9-p16 MIS into SP-53 cells without transporter or by the indicated transporters; SP-53 cells (2×10^5), FITC-labeled r9-p16 MIS (final concentration, 2 μmol/L), Wr-T (5 μmol/L). Cellular uptake in living SP-53 cells (*left*). Comparison of transduction efficiency between Pep-1 and Wr-T (*right*). FITC-r9-p16 MIS (2 μmol/L), Pep-1 (20 μmol/L), and Wr-T (5 μmol/L). Cells were examined at the indicated time point after peptide introduction. Propidium iodide was used for nuclear staining. **C,** FACS analysis for cellular uptake of FITC-r9-p16 MIS in SP-53 for the indicated transporters 12 hours after introduction (*left*) and the transduction efficiencies for each method (*right*). Pep-1 (20 μmol/L), WR-T (all ''R'' composed of L-arginines, 5 μmol/L), Wr-T (all ''r'' composed of D-arginines, 5 μmol/L), FITC-labeled r9-p16 MIS (2 μmol/L), respectively. *Columns,* the mean fluorescence intensity of each sample using the intensity of the r9-p16 MIS – treated cells as a standard. Background fluorescence intensity (the intensity of untreated cells) was 0.02.

which the Wr-T transporter system was the most efficient. Wr-T showed the maximum efficiency, which was 15 times more than the single r9-p16 MIS peptide and 25 times more than the Pep-1 transporter (Fig. 1C). WR-T, with a protein transduction domain composed of nine L-arginine residues, enabled r9-p16 delivery at elevated, although not the very highest, efficiencies.

Intracellular Localization and Function of the p16 MIS Peptide Delivered by Wr-T

We next determined whether the p16 peptide was delivered by Wr-T as a functional peptide to target cell cycle–regulated molecules in SP-53 cells. Confocal microscopic analysis revealed that Wr-T delivered substantial amounts of r9-p16 MIS into the nucleus (Fig. 2A, *left*). We visualized nuclear localization in the XZ plane (Fig. 2A, *arrows, right*). In the images of the assembled sections, yellow signals were detected in nuclei of cells treated with Wr-T/r9-p16 MIS mixture but not in nuclei of cells treated with Wr-T alone. Thus, Wr-T is necessary for heightened nuclear delivery of r9-p16 MIS, and neither Wr-T alone (Fig. 2A) nor r9-p16 MIS alone was effective (Fig. 1B). Because R9-fused peptides are known to accumulate within the endosomes and they eventually escape from there by disrupting lipid bilayers (16), it is possible that enhanced uptake of r9-p16 MIS by Wr-T promotes the release/redirection of much of the endosomally accumulated cargo

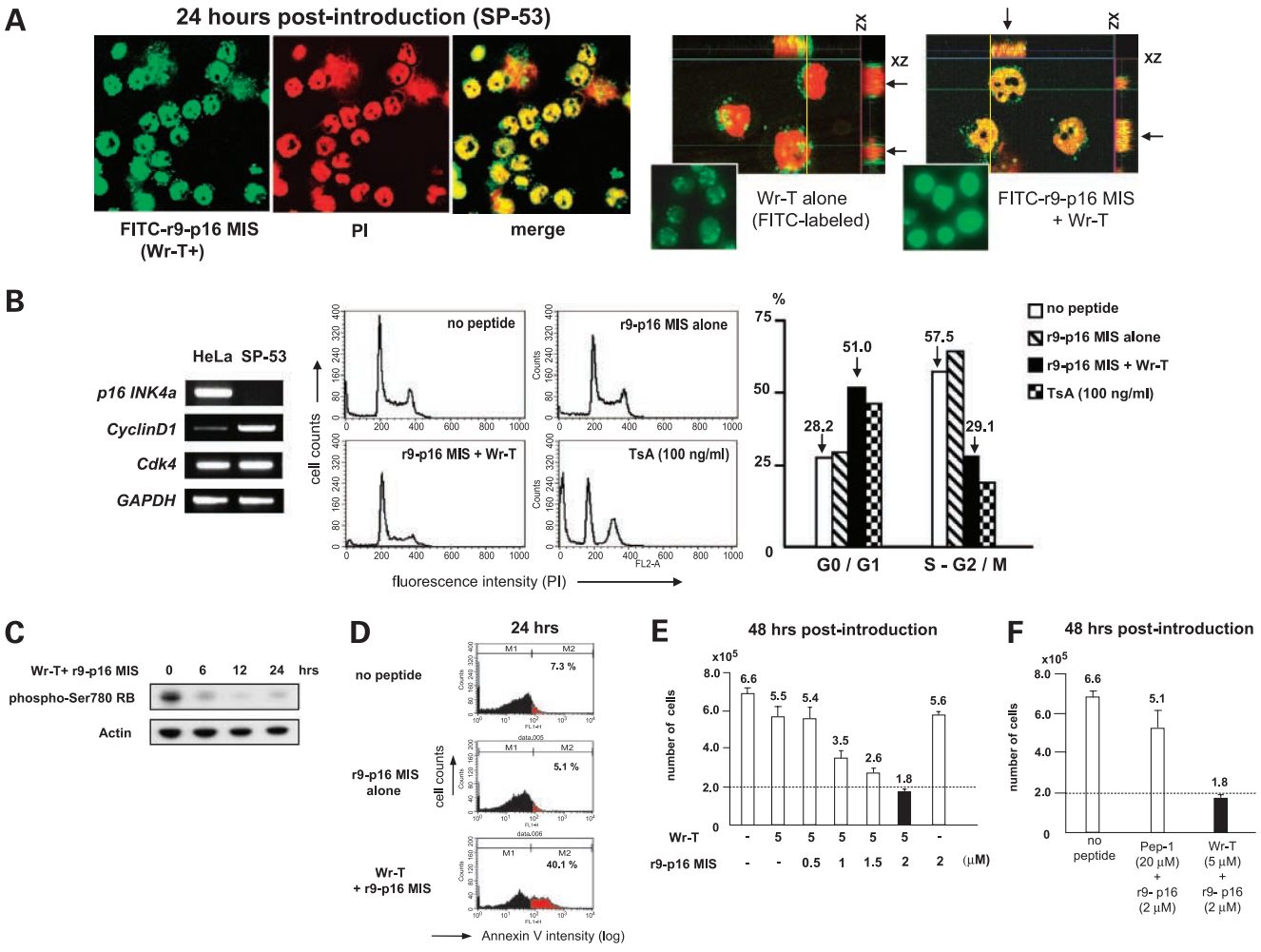

Figure 2. Functional analysis of intracellularly targeted r9-p16 MIS using Wr-T. **A,** intracellular localization of FITC-r9-p16 MIS (2 μmol/L) delivered by Wr-T (5 μmol/L, *left*). *PI,* propidium iodide; *merge,* both were colocalized. Sectional images of the cells along the XZ plane (*right*). *Arrows,* vertically sectioned cells. *Insets,* living cells treated with FITC-Wr-T alone (*left*); living cells treated with FITC-r9-p16 MIS + Wr-T (*right*). **B,** enlarged G_0-G_1 phase in cells treated with Wr-T/r9-p16 MIS mixture. Expression analysis of p16-related genes in SP-53 cells by reverse transcription-PCR (*left*), cell cycle analysis of propidium iodide–stained cells by FACS (*middle*), and summary of cell cycle analyses (*right*). Cells treated with trichostatin A, which blocks the cell cycle at G_0-G_1, were used for comparison. **C,** reduced expression of phospho-Ser^{780} pRB in Wr-T/r9-p16 MIS–introduced cells assessed by immunoblotting (Wr-T, 5 μmol/L; r9-p16 MIS, 2 μmol/L). **D,** FACS analysis using Annexin V 24 hours after peptide treatment. Percentage of Annexin V positive cells depicted in *red*. **E,** dose-dependent growth suppression of SP-53 cells transduced with Wr-T/p16 MIS complexes. **F,** efficiencies of growth suppression from transduction with Pep-1/r9-p16 MIS complexes and Wr-T/r9-p16 MIS complexes. (Initial number of cells, 2.0×10^5).

peptide. This would help explain the nuclear localization observed in the present study, although a precise mode of action for Wr-T in regulating traffic of a cargo peptide remains unclear. At 24 hours post-transduction, FACS analysis with propidium iodide staining showed that the SP-53 cells incubated with the Wr-T/r9-p16 MIS mixture preferentially accumulated at the G_0-G_1 (51.0%) phase, compared with mock-treated cells (28.2%) and cells treated only with r9-p16 MIS (29.1%). This result was similar to that obtained with cells treated with trichostatin A, a cell cycle inhibitor at G_0-G_1 (Fig. 2B, *middle*). Because arrest in G_1 phase is expected to abrogate phosphorylation of pRB, we investigated the practical effect of Wr-T–mediated r9-p16 MIS delivery on cell cycle–related pRB status (17, 18). By 6 hours post-transduction, phosphorylated pRB (Ser^{780} phosphorylation) was dramatically decreased in the cells containing Wr-T/r9-p16 MIS mixture, consistent with the induction of cell cycle arrest by the introduced p16 MIS (Fig. 2C). Approximately 40% of these cells were Annexin V positive at 24 hours post-transduction, suggesting that the nuclear r9-p16 MIS had triggered apoptosis (Fig. 2D). Taken together, these findings indicate that the Wr-T is critical for efficient delivery of target peptide (protein) to the nucleus and that the transduced peptide, r9-p16 MIS, is actually functional within these cells. Wr-T–transported r9-p16 MIS inhibited SP-53 cell growth in a dose-dependent manner, whereas r9-p16 MIS alone did not significantly suppress growth (Fig. 2E). Comparing the efficiency of inhibition by the Wr-T/r9-p16 MIS mixture to that by the Pep-1/r9-p16 MIS after 48 hours, SP-53 growth inhibition associated with Wr-T delivery (73%) was much greater than that resulting from Pep-1 delivery (23%; Fig. 2F).

Growth Inhibition of Leukemia/Lymphoma Cells by the Wr-T/r9-p16 Transduction System

Based on these results, we attempted to suppress growth of biologically aggressive leukemia/lymphomas (19–21) using the Wr-T–transported r9-p16 MIS. With the exception of acute B-cell lymphoblastic leukemia "BALL-1," such leukemia/lymphoma cells lack *p16* mRNA expression (Fig. 3A, *left*). Consistent with this nonexpression, multiple phosphorylated forms of pRB including Ser^{780} were detected in these cells, indicating pRB inactivation along with accelerated cell proliferation (Fig. 3A, *right*). We introduced r9-p16 MIS into this background by mixing each neoplastic line with Wr-T (final concentration: Wr-T, 5 μmol/L; r9-p16 MIS, 2 μmol/L) and monitoring cell proliferation, starting with 2.0×10^5 cells per incubation. With the exception of BALL-1, which expresses *p16*, all tumor lines incubated with Wr-T/r9-p16 MIS mixture showed dramatic suppression of cell proliferation

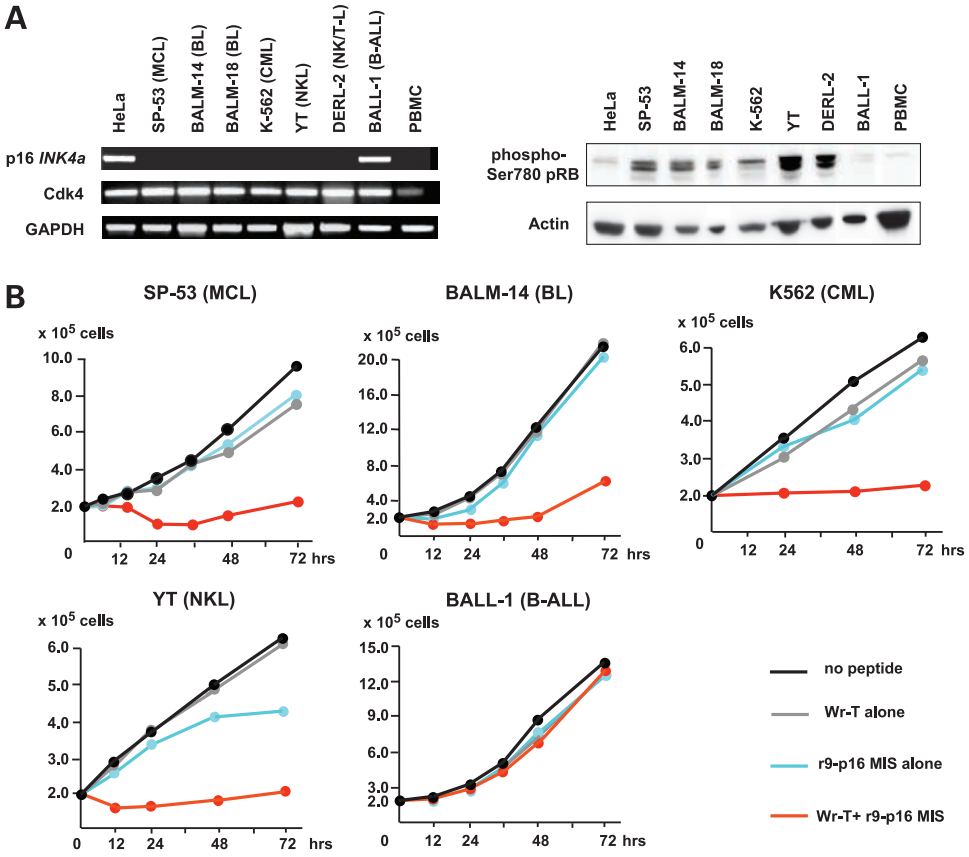

Figure 3. Growth suppression of lymphoma/leukemia cell lines by Wr-T transporter system. **A,** mRNA expression of $p16^{INK4a}$, Cdk4, and GAPDH in lymphoma/leukemia cell lines using reverse transcription-PCR (*left*). Endogenous expression of phospho-Ser^{780} pRB in the examined cell lines by immunoblotting (*right*). *MCL*, mantle cell lymphoma; *BL*, Burkitt's lymphoma; *B-ALL*, acute B-cell leukemia; *CML*, chronic myelocytic leukemia; *NKL*, natural killer cell lymphoma; *NK/T-L*, natural killer/T-cell lymphoma. **B,** cell growth suppression by transduction of Wr-T/r9-p16 MIS complexes (Wr-T, 5 μmol/L; p16 MIS, 2 μmol/L). Five representative cases of leukemia/lymphoma cell lines are shown. The numbers of cells treated with the Wr-T/r9-p16 MIS mixture were compared with those of cells without peptides, with Wr-T (5 μmol/L) alone, and with r9-p16 MIS (2 μmol/L) alone (initial cell number, 2.0×10^5).

(Fig. 3B). In contrast, administration of r9-p16 MIS alone yielded no significant growth suppression in any of these cell lines; presumably, the lack of BALL-1 growth suppression for any of the treatments is due to the growth independence of this line from the Cdk4-p16-RB signaling pathway. The Wr-T/r9-p16 MIS delivery system should therefore be quite useful for inhibiting a spectrum of p16-negative, but not p16-positive leukemia/lymphoma lines. To examine the biological effect of this Wr-T/p16 delivery system against nonneoplastic lymphocytes was considered to be important, we examined whether the Wr-T/r9-p16 MIS complexes adversely affect the viability of PBMCs from healthy donors. At either 24 or 48 hours, we observed only a slight cytotoxicity of <5% in these PBMCs for the same concentration of mixture used with the leukemia/lymphoma cells. This negligible cytotoxicity to PBMCs is not due to differential uptake because >98% of the PBMCs had internalized r9-p16 MIS (data not shown).

Advanced Applications of the Wr-T/p16 Transduction System

We next determined if the p16 delivery system was effective on primary lymphoma cells directly isolated from patients. We obtained primary lymphoma cells from a patient's pleural effusion (Fig. 4A, *left*), and treated with Wr-T/r9-p16 MIS mixture. These cells do not express p16 (Fig. 4A, *top left*), carry the t(8;14)(q24;q32) translocation, nor have a B-cell phenotype (data not shown). Fluorescence microscopic and FACS analyses showed enhanced cellular uptake of FITC-r9-p16 MIS in the presence of Wr-T in >97% of the living cells (Fig. 4A, *middle*). After 24 and 48 hours of incubation, FACS analysis further indicated that the incorporated peptide inhibited growth and induced apoptosis, with efficiency greater than the single r9-p16 MIS treatment (Fig. 4A, *right graph*).

Because conceivably, Wr-T–based delivery system could have therapeutic uses, we established animal tumor

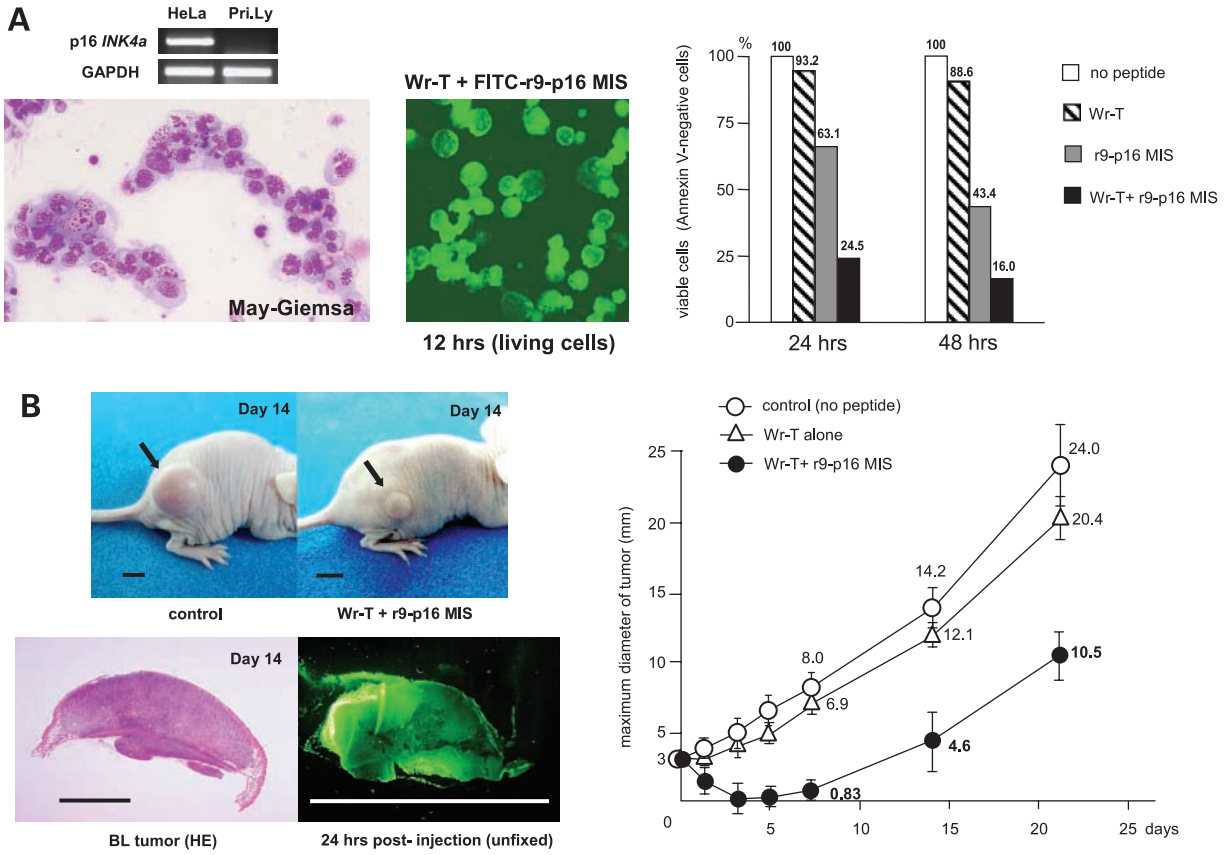

Figure 4. Use of Wr-T/r9-p16 for primary lymphoma and *in vivo* tumors. **A,** application of the Wr-T/ r9-p16 MIS delivery system on primary lymphoma cells. Primary lymphoma cells (2.0×10^5) lacking *p16* expression were introduced with r9-p16 MIS (2 μmol/L) by Wr-T (5 μmol/L). Cytology by May-Giemsa staining (*left*) and intracellular uptake of FITC-r9-p16 MIS (*middle*). *Columns,* percentages of viable cells in each indicated sample relative to those in untreated cells 24 and 48 hours after introduction as determined by FACS analyses using Annexin V (*right*). *Pri.Ly*, primary lymphoma cells. **B,** inhibition of tumor growth by single administration of Wr-T/r9-p16 MIS mixture in mouse model transplanted with Burkitt's lymphoma cells. *Arrows*, tumors at 14 days after each treatment (*top left*, control PBS; *top right*, Wr-T/r9-p16 MIS mixture). Histology of the s.c. tumor (H&E stain, *bottom left*), uptake of FITC-r9-p16 MIS by Wr-T in frozen, sectioned Burkitt's tumor (*bottom right*). Bar, 5 mm. Tumor growth curve by single treatment with a mixture of Wr-T and r9-p16 (*right graph*). Maximum diameters of tumors in each group (no peptide group: $n = 3$; Wr-T group: $n = 3$; Wr-T/p16 group: $n = 3$) were measured at the indicated time.

models by s.c. injection of human Burkitt's lymphoma cells, BALM-14, into BALB/c nude mice (Fig. 4B). When tumors grew to ~3 mm, we injected the Wr-T/r9-p16 MIS mixture so as to surround the whole tumor and measured tumor growth over time, comparing tumor sizes with untreated tumors (Fig. 4B, *top*). Twenty-four hours post injection, the FITC-r9-p16 MIS of the peptide mixture had become widely distributed throughout the tumor (Fig. 4B, *bottom right*). Within the first week, decreases in tumor size were evident in the mice treated with a single application of the peptide mixture, whereas the peptide-free tumors grew to thrice their initial size (Fig. 4B, *right graph*). Therefore, only a single treatment with transducible Wr-T/r9-p16 complexes suffices to significantly retard the mouse tumor growth.

Discussion

There still remains a host of aggressive leukemia/lymphomas recalcitrant to the therapies currently available. One of the genetic hallmarks of such malignancies is the frequent nonexpression of tumor suppressor $p16^{INK4a}$. Although the recently reported protein transduction domain transduction systems have gained considerable attention for their therapeutic delivery potential, their present efficiencies fall short of the practical requirements. Consequently, we have introduced a novel transporter system for delivering cargo peptide to hematopoietic cells with unprecedented efficiency; transduction of functional p16 peptide by our method drastically inhibited the growth of aggressive leukemia/lymphoma cells. Concretely, the following results have been achieved through the present study; Wr-T dramatically enhanced intracellular uptake of a cargo peptide into hematopoietic cells including primary lymphoma cells, and it enabled diffusion of a cargo peptide throughout a whole cell. The delivered cargo peptide by Wr-T was shown to specifically function in the targeted cells. Moreover, this p16 delivery system functioned only in p16-negative aggressive leukemia/lymphomas, not block proliferation of p16-expressing tumor cells nor PBMCs, which indicates its selectivity for practical use. Thus, our results provide a framework for significantly advancing the molecular targeting of intractable hematopoietic malignancies.

Other molecular targeting approaches for hematopoietic malignancies have been reported, such as the use of the RI-TAT p53C′ peptide against Burkitt's lymphoma (22). In that work, a 48 hour treatment with 20 to 30 μmol/L of peptide for targeting the p53 protein inhibited growth of ~50% of the lymphoma cells. Their system also showed success with s.c. developed breast carcinoma and peritoneally disseminated Burkitt's lymphoma under a regimen of 16 times injections of peptide. In our present study, the p16 peptide delivered by Wr-T was effective at concentrations as low as 2 μmol/L for several cases of leukemia/lymphomas *in vitro* and *in vivo*. Moreover, a single administration of the Wr-T/r9-p16 MIS mixture strongly inhibited the growth of lymphoid tumor *in vivo*.

In conclusion, the Wr-T transporter system enables highly efficient and specific peptide delivery to hematopoietic neoplasms, yielding the most pronounced reductions in tumor cell growth seen thus far with this class of interventions. In this sense, this system may be of more practical use for a peptide therapy than the previous protein transduction domain systems and offers the additional convenience of choice in cargo peptides, as well as the potential for being adapted to regimens involving multiple administrations or being combined with other antitumor agents. We hope the continued development of the Wr-T–based protein docking strategy will increase the success rate in combating the particular neoplasms we have studied.

Acknowledgments

We thank Y. Matsuo, A. Harashima, and T. Teshima for providing us with leukemia/lymphoma cell lines; S. Suzuki for the gift of antiserum to human phospho-Ser^{780} pRB; K. Isomoto, Y. Onoda, T. Miyake, and T. Tanaka for their technical support; and I-W. Park and K. V. Myrick for critical reading of the manuscript.

References

1. Nagahara H, Vocero-Akbani AM, Snyder EL, et al. Transduction of full-length TAT fusion proteins into mammalian cells: TAT-p27Kip1 induces cell migration. Nat Med 1998;4:1449–52.

2. Derossi D, Joliot AH, Chassaing G, Prochaintz A. The third helix of the Antennapedia homeodomain translocates through biological membranes. J Biol Chem 1996;269:10444–50.

3. Wender PA, Mitchell DJ, Pattabiraman K, et al. The design, synthesis, and evaluation of molecules that enable or enhance cellular uptake: peptoid molecular transporters. Proc Natl Acad Sci U S A 2000;97:13003–8.

4. Fisher PM, Krausz E, Lane DP. Cellular delivery of impermeable effector molecules in the form of conjugates with peptides capable of mediating membrane translocation. Bioconjug Chem 2001;12:825–41.

5. Joliot A, Prochiantz A. Transduction peptides: from technology to physiology. Nat Cell Biol 2004;6:189–96.

6. Morris MC, Depollier J, Mery J, Heitz F, Divita G. A peptide carrier for the delivery of biologically active proteins into mammalian cells. Nat Biotechnol 2001;19:1173–6.

7. Fahraeus R, Lain S, Ball KL, Lane DP. Characterization of the cyclin-dependent kinase inhibitory domain of the INK4 family as a model for a synthetic tumour suppressor molecule. Oncogene 1998;16:587–96.

8. Daibata M, Kubonishi I, Eguchi T, et al. The establishment of Epstein-Barr virus nuclear antigen-positive (SP-50B) and Epstein-Barr virus nuclear antigen-negative (SP-53) cell lines with t(11;14)(q13;q32) chromosome abnormality from an intermediate lymphocytic lymphoma. Cancer 1989;64:1248–53.

9. Drexler HG, editor. The leukemia-lymphoma cell line factsbook. San Diego (CA); Academic Press: 2000.

10. Hiraki S, Miyoshi I, Kobonishi I, Matsuda Y. Establishment of an Epstein-Barr virus-determined nuclear antigen-negative human B-cell line from acute lymphoblastic leukemia. J Natl Cancer Inst 1977;59:93–4.

11. Matsuo Y, Drexler HG. Immunoprofiling of cell lines derived from natural killer-cell and natural killer-like T-cell leukemia-lymphoma. Leuk Res 2003;27:935–45.

12. Fink JR, LeBien TW. Novel expression of cyclin-dependent kinase inhibitors in human B-cell precursors. Exp Hematol 2001;29:490–8.

13. Hangaishi A, Ogawa S, Imamura N, et al. Inactivation of multiple tumor-suppressor genes involved in negative regulation of the cell cycle, MST1/p16INK4A/CDKN2, MST2/p15INK4B, p53, and Rb genes in primary lymphoid malignancies. Blood 1996;87:4949–58.

14. Herman JG, Civin CI, Issa JP, et al. Distinct patterns of inactivation of p15INK4B and p16INK4A characterize the major types of hematological malignancies. Cancer Res 1997;57:837–41.

15. Drexler HG. Review of alterations of the cyclin-dependent kinase

inhibitor INK4 family genes. P15, p16, p18, and p19 in human leukemia-lymphoma cells. Leukemia 1998;12:845 – 59.

16. Fuchs SM, Raines RT. Pathway for polyarginine entry into mammalian cells. Biochemistry 2004;43:2438 – 44.

17. Medema RH, Herrera RE, Lam F, Weinberg RA. Growth suppression by $p16^{ink4a}$ requires functional retinoblastoma protein. Proc Natl Acad Sci U S A 1995;92:6289 – 93.

18. Tamraker S, Rubin E, Ludlow JW. Role of pRB dephosphorylation in cell cycle regulation. Front Biosci 2000;5:121 – 37.

19. Hiddemann W, Longo DL, Coiffier B, et al. Lymphoma classification—the gap between biology and clinical management is closing. Blood 1996; 88:4085 – 9.

20. Muller-Hermelink HK, Zettl A, Pfeifer W, Ott G. Pathology of lymphoma progression. Histopathology 2001;38:285 – 306.

21. Howard AM, Shipp MA. The cellular and molecular heterogeneity of the aggressive non-Hodgkin's lymphomas. Curr Opin Oncol 1998;10: 385 – 91.

22. Snyder EL, Meade BR, Saenz CC, Dowdy SF. Treatment of terminal peritoneal carcinomatosis by a transducible p53-activating peptide. PLoS Biol 2004;2:186 – 93.